

RESEARCH ARTICLE

Characteristics of dual media in tight-sand gas reservoirs and its impact on reservoir quality: A case study of the Jurassic reservoir from the Kuqa Depression, Tarim Basin, Northwest China

Pengwei Wang¹  | Zhijun Jin¹ | Xiongqi Pang² | Yingchun Guo³ | Xiao Chen⁴ | Hong Guan⁴

¹Research Institute of Petroleum Exploration & Production, SINOPEC, Beijing, China

²College of Geosciences, China University of Petroleum, Beijing, China

³Institute of Geomechanics, Chinese Academy of Geological Sciences, Beijing, China

⁴CNOOC research institute, Beijing, China

Correspondence

Yingchun Guo, Institute of Geomechanics, Chinese Academy of Geological Sciences, Beijing, China.

Email: 294560512@qq.com

Funding information

China Postdoctoral fund, Grant/Award Number: 2017M610150; China National Science and Technology Major Project, Grant/Award Number: 2016ZX05047-006

Handling Editor: Z.-Q. Chen

The recent gas exploration in West China demonstrated that formation conditions of tight-sandstone gas are distinct from typical ones in North America. One remarkable difference is that complicated tectonic conditions in the foreland basin of West China, especially the Himalayan tectonic movement, resulted in widely developed fractures in tight-sand reservoirs. Thus, this work employed dual media to characterize tight-sand reservoir system and explain the impact of dual media on tight-sand gas reservoir by: (a) describing the feature of fractures and properties of Yinan 2 tight-sand reservoir; (b) characterizing dual media with mercury intrusion porosimetry, full diameter and conventional core analysis; (c) discussing gas charging and accumulating in dual media based on the difference between dual media and tight-sand rocks. Observation from cores, FMI images and thin sections suggested that macro- and micro-fractures are widely distributed in Lower Jurassic Ahe Formation (J₁a) tight sandstones, with dip angle of 70° to 80°. These fractures are strongly scale-dependent with length of several centimetres to a few tens of centimetres and apertures of several hundreds to several thousands of microns. J₁a tight-sand reservoir is characterized by poor porosity, with an average value of 7.7%, whereas measured permeability varies from 0.01–100 mD. Intrusion and extrusion curves of dual media and tight-sand rocks are significantly different from each other, while displacement pressure and medium saturation pressure of dual media are lower than tight-sand rocks. Importantly, maximum pore throats of dual media are 1.75–32.22 times larger than juxtaposed tight-sand rocks. The ratio of permeability between dual media and tight sandstone is up to 1,000, whereas the ratio of porosities only ranges from 1 to 1.5. Thus, dual media in tight-sand reservoir represents high permeability system and matrix pores are primarily storage system. The impact of dual media on tight-sand gas reservoir involves its position, temporal coupling of gas charging and growth. In terms of fracture growth prior to gas charge, multi-force can work together as a driving force, and fractures as a flow system and matrix pores as a storage system linked by fractures; buoyancy is the primary driving force in fractures. In terms of gas charge prior to fracture growth, dual media can also exert a positive impact on gas charging when occurring in the inner part of tight-sand reservoir defined by the critical throat threshold. However, dual media can also destroy the “inverted gas–water” and shrink tight-sand gas reservoir when occurring at the original critical throat threshold.

KEYWORDS

fracture growth, gas charging, Mesozoic, properties, tight-sand rocks

1 | INTRODUCTION

As global demand for natural gas intensifies, identifying and producing reserves from ultra-low-permeability (nanodarcys) and low-porosity (<12%) reservoirs have gained worldwide exploration interest and activity. One such unconventional gas system is the continuous tight-sand gas reservoir, such as Cretaceous sandstone reservoirs of Western Alberta, Jonah field in Green River Basin, the San Juan Basin in New Mexico, and Wattenberg field in the Denver Basin of Colorado. Of all classification principles of tight sand gas reservoirs (Wei et al., 2016), the continuous tight-sand gas (or basin-centred gas) is the most common and valuable type (Dai, Ni, & Wu, 2012), which are typically characterized by: (a) large regional distribution, (b) very low reservoir porosity and permeability with strong heterogeneity, (c) abnormal pressure, (d) no down dip water leg, and (e) regionally pervasive gas-saturated reservoirs instead of trap structures. Considerable tight-sand gas resource has been discovered in China petroliferous basins, such as those in Sichuan Basin, Ordos Basin, and Songliao Basin (Dai et al., 2012; Zou et al., 2013). Success in producing gas from these potential tight-sand gas reservoirs made it currently an important emerging source for gas supply in China (Jia, Zheng, & Zhang, 2012; Zou et al., 2012).

Previous studies suggested that tight sandstones were dominated by nano-scale (pore diameter < 1 mm) to micro-scale pores (Bai et al., 2013; Desbois, Urai, Kukla, Konstanty, & Baerle, 2011; Hinai, Rezaee, Esteban, & Labani, 2014; Rezaee, Saeedi, & Clennell, 2012), and tight-sand reservoir quality was mainly governed by pore-throat geometry and pore-network, such as pore-types, shapes, size, and distribution of pores and throats as well as their connectivity (Shanley & Cluff, 2015). Various explanations, including well-known water block (Masters, 1979), relative permeability block or permeability jail (Cluff, Shanley, & Byrnes, 2005), lack of buoyancy (Gies, 1981), and stratigraphic-diagenetic trapping (Cant, 1983; Zhang et al., 2009), have been proposed to explain trapping mechanisms of tight-sand gas. Also, several physical modelling experiments have been conducted on piston-forwarding gas-water inversion accumulation (Gies, 1984; Pang, Jin, & Jiang, 2003; Xiao, Zhong, Huang, Jiang, & Liu, 2008). These experiments demonstrated that gas-water inversion could form and remain under certain conditions.

However, different from these typical continuous tight-sand gas reservoir in North America, natural fractures are well-developed in tight sands and play important role in successful and economic production of gas from tight-sand reservoirs in the foreland basin in the Tarim Basin, Northwest China. For example, tight-sand reservoirs in the western Sichuan Depression of the Sichuan Basin and Kuqa Depression of the Tarim Basin generally experienced complicated tectonic movements, especially the Himalayan tectonic movement, which resulted in wide fracture growth in tight sand reservoirs (Zeng & Liu, 2006; Zeng, Wang, Gong, & Liu, 2010). These tectonic fractures can be shear or extension fractures and are strongly scale-dependent, which tend to be pervasive from large scale to grain-size scale.

The growth of fracture in tight-sand reservoir strongly influences rock properties, flow capacity, gas charging and accumulation, and furthermore the development of sweet spots and gas production in tight sand reservoir (Anovitz et al., 2013; Coskun & Wardlaw, 1996;

Lyu et al., 2017; Shanley & Cluff, 2015; Zhao et al., 2015). Previous studies from Aguilera (1995) and Landes (1959) classified fractured reservoirs into three types based on their storage property, including Type A, B, or C. In reservoir of Type A, the primary hydrocarbon storage is matrix pores and a small amount of storage is in fractures. This is the case of tight-gas sands where fractures provide the necessary permeability allowing gas flow. In reservoirs of Type B, matrix pores and fractures are equally important for hydrocarbon storage, whereas, tight rocks are impermeable and fractures are much more permeable than the matrix. In reservoir of Type C, all hydrocarbon storage is from fractures with no contribution from matrix pores. In this condition, fractures provide both storage space and the necessary permeability required to achieve commercial production.

The existence of fractures makes it difficult to characterize pore network and evaluate tight-sand in such a reservoir quality. Also, gas accumulation mechanism in a such reservoir is crucial yet very poorly understood, and exploration preformation on these unconventional reservoirs are therefore challenging.

The dual porosity was originally proposed to study the typical behaviour of a permeable medium that contribute significantly to the pore volume but contribute negligibly to the flow capacity, for example, a vugular reservoir in carbonate reservoir (Chilingar, Mannon, & Rieke, 1972). Yang (2004) put forwarded dual media model to describe the characteristic of the combined inter-granular, inter-crystalline, vuggy, and fracture in carbonate rocks, which can work as dual, triple, and even multi-porosity and multi-permeability behaviour. Chen et al. (2017) defined a dual-porosity model to describe and treat separately organic pores and matrix pores in shale reservoirs. Similarly, fractures and pores can give origin to dual-porosity or dual-permeability behaviour in a tight-sand reservoir. Thus, this work attempted to employ the dual media model to identify the characteristics of combined fracture and matrix pores in a fractured tight-sand reservoir and discuss its impact on tight-sand gas reservoir. First, fractures in tight-sand reservoir were described with core observation, FMI images and thin sections, and general petrophysical properties were illustrated with available data from core analysis. The dual media in Yinan 2 tight-sand reservoir was characterized through full diameter core analysis and conventional core analysis and pressure-controlled mercury injection. Finally, we discuss the impact of the dual media model on the accumulation of continuous tight-sand gas.

2 | GEOLOGICAL SETTING

The Kuqa Depression, a typical foreland sub-basin, is located on the northern margin of the Tarim Basin, NW China with a width of 30–80 km from south to north and a length of 550 km from west to east (Figure 1). The Tarim Basin, lying in the southern Xinjiang Province, NW China and is surrounded by the Kunlun, Tien Shan, and Altyntagh mountains to the south, north, and southeast, respectively (Figure 1). The basin is the largest hydrocarbon-resourcing basin in China. Tectonically, the Tarim Basin is separated on the south from the Kunlun fold belt by the Kunlun Mountain frontal suture and the Altyntagh Deep fault and on the north from the Tien Shan fold belt and the Turpan-Hami Basin by the southern Tien Shan suture and the northern Kuruktagh

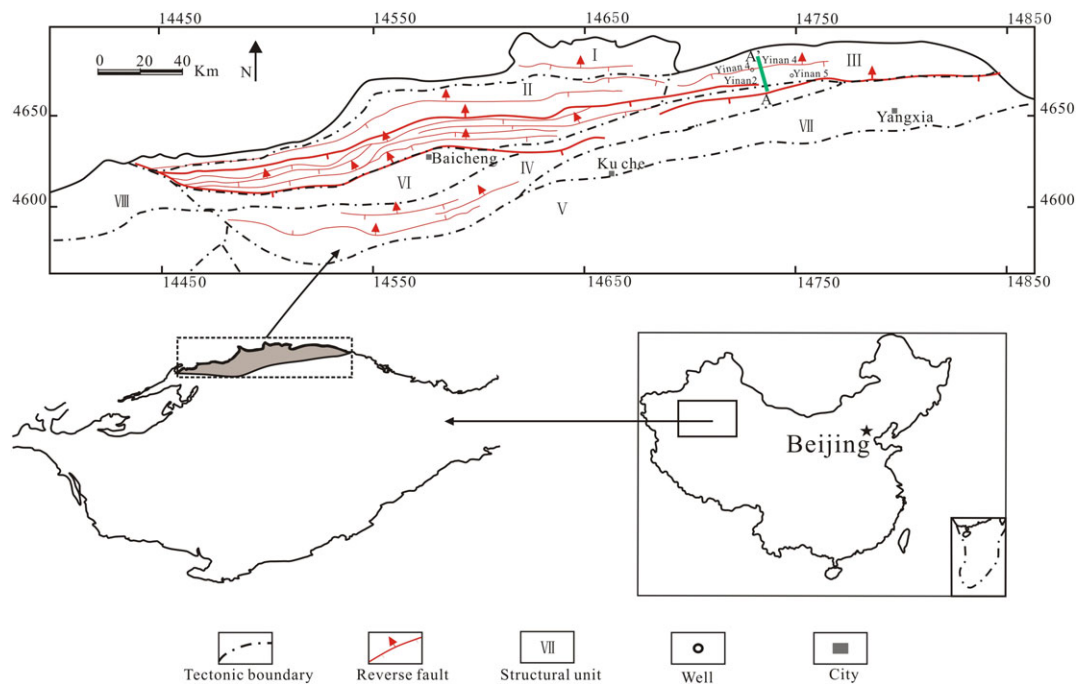


FIGURE 1 Location map of the study area showing the sub-tectonic units of Kuqa Depression within the Tarim Basin, Western China. I: The northern monocline belt, II: The Kelasue structural belt, III: The Yiqikelike structural belt, IV: The Qiulitage structural belt, V: The frontal uplift belt, VI: The Baicheng Sag, VII: The Yangxia Sag, and VIII: The Wushi Sag. The A-A' section in the Yiqikelike structural belt in Figure 4 is also shown. This section is across the Yinan 2 tight-sand gas reservoirs that include wells Yinan 2, Yinan 4, Yinan 5, and Yishen 4 [Colour figure can be viewed at wileyonlinelibrary.com]

Fault (Chen & Shi, 2003; Jia, 1997; Jia, Lu, & Cai, 1998; Yin et al., 2002; Yin & Harrison, 2003). For the purpose of hydrocarbon exploration, this basin is subdivided into the Tazhong Uplift, Tabei Depression, Southwest Sag, Kuqa Depression, North Depression, South Uplift, and Southeast Depression (Jia et al., 1998). Of these, the Kuqa Sag is filled with the Mesozoic–Cenozoic sediments and is rich in gas resource.

Generally, the structure in the Kuqa Depression is dominated by thrust faults and folds developing during the Cenozoic. In a map view, the Kuqa Depression consists of four structural belts and three sags, including the northern monocline belt, the Kelasue structural belt, the Yiqikelike belt, the Qiulitage structural belt, the Frontal uplift belt, the Baicheng Sag, the Yangxia Sag, and the Wushi Sag (Figure 1; Chen, Tang, Jin, Jia, & Pi, 2004; Fan, Lu, Yang, & Xie, 2008; Fu, Song, Lü, & Sun, 2006; Liu et al., 2000; Tang et al., 2004; Wang, 2002). Although the Kuqa Depression has experienced multiphase tectonic movements, the Himalayan tectonic movement was responsible for the common structural style of the study area (Ding & Luo, 2005; Gao & Zhao, 2001; Zeng, 2004).

The strata in the Kuqa Depression primarily consist of the Mesozoic and Cenozoic sequences (Figure 2). Source rocks in the Kuqa Depression primarily are distributed in the Middle–Upper Triassic and Lower–Middle Jurassic (Gao & Zhao, 2001). Middle–Upper Triassic source rocks include the Middle–Upper Karamay Formation (T_{2-3k}), the Huangshanjie Formation (T_{3h}), and the Taliqike Formation (T_{3t}). Dominated by Type III kerogens, source rocks in Middle–Lower Jurassic and Upper–Middle Triassic are rich in organic matter, with the average TOC of 3.18 and 2.62 wt.%, respectively. Importantly, source rocks are within the gas-window, with reflectance of 1.3–1.4% and 1.1–1.4%, respectively in the Yinan 2 well.

Tight sands were widely spread in Paleogene, Cretaceous, and Jurassic, and the Lower Jurassic Ahe Formation (J_{1a}) is regarded as primary tight-sand reservoirs. The J_{1a} can be divided into four members vertically from bottom to top, including first, third, and fifth members (J_{1a}^1 , J_{1a}^2 , J_{1a}^3 , and J_{1a}^4). J_{1a}^1 , J_{1a}^3 , and J_{1a}^4 are primarily light-grey poor-sorted sandstones, which were deposited in the braided river delta setting with a total thickness of 199.5 m. The J_{1a} tight-gas reservoirs are dominated by lithoclastic and quartz. The reservoir was characterized by secondary solution pores and minor primary pores, with porosity generally less than 8% and permeability less than $1 \times 10^{-3} \mu\text{m}^2$.

Taliqike Formation (T_{3t}) source rocks and Ahe Formation (J_{1a}) tight-sand reservoirs are in close proximity continuous tight-sand gas. And evidences has dominated that the Yinan 2 tight-sand gas was primarily sourced from T_{3t} source rocks (Zou, Jia, Tao, & Tao, 2011). For example, Ro values converted from $\delta^{13}\text{C}_1$ are 0.94–1.45%, whereas the Ro values from T_{3t} source rocks is as high as 2.26% (Gu, Zhu, & Jia, 2003). Natural gas from Yinan 2 tight-sand reservoirs is characterized by relative low density (0.6283–0.6335), high methane content (88.6104–89.4456%), which gas reservoir is normal temperature and ultra-high pressure (116–135 °C, 68.5 9–81.34 MPa).

3 | DATA AND METHOD

A total of 32 core samples from four wells (Yinan 2, Yinan 4, Yinan 5, and Yishen 4 wells) was observed, and more than 80 thin sections and one FMI image from Dixi 1 well were obtained from Research Institute of Petroleum Exploration and Development of the Tarim Oilfield Company, PetroChina, which were combined to describe the

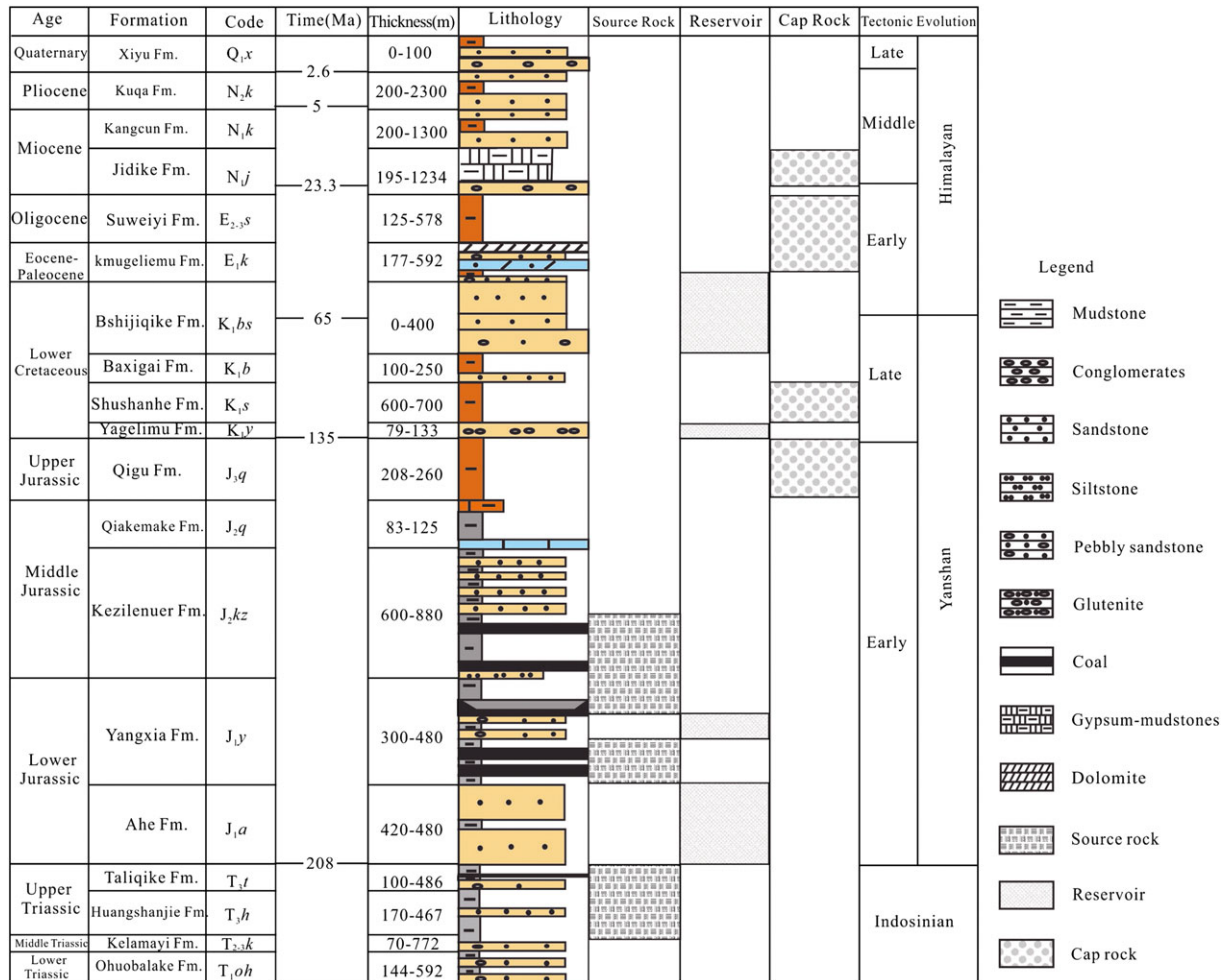


FIGURE 2 Schematic stratigraphy of the Kuqa Depression showing petroleum system elements and tectonic evolution stages, including T_{2-3k}, T_{3h}, T_{3t}, J_{1y}, and J_{2kz} source rocks, J_{1a} and other multiple reservoir intervals, cap rocks, J_{1a} as well (modified from Zeng et al., 2010) [Colour figure can be viewed at wileyonlinelibrary.com]

growth of fractures in tight-sand reservoir in different scale. In addition, reservoir porosity and permeability of 1,536 available data were collected to generally describe the rock property in Yinan 2 tight-sand reservoir.

To reduce the biased estimate caused by heterogeneity, this paper selected fractures and juxtaposed none-fracture samples (mostly within 1 m) to conduct experiments.

Full diameter core analysis and conventional core analysis were used to compare the petrophysical property of dual-media samples and tight-sand samples and discuss the contribution of fractures to reservoir quality. Conventional core analysis is commonly used to analyse matrix porosity and permeability in tight-sand rocks, because sampling makes it difficult to contain fractures in samples. Also, limited by sample size, it can only reflect the local rock property of cores. A total of 18 none-fractured samples were used to perform conventional core analysis using SL-5 rock permeability analyser. It was done with a temperature and pressure of 24 °C and 91.5 kPa, respectively, following the standard SY/T 5336-1996 of China. However, full diameter core analysis can describe the heterogeneity caused by fractures and dissolution pores of the whole cores and calculate rock property accurately. Specifically, another 18 juxtaposed fractured-samples from four wells were selected and cut into cylinders with 65, 100, and

120 mm in diameter and about 20-130 mm in length. Importantly, both ends of the sample are required to be perpendicular to the axis, with the error less than 0.02 mm. Samples were washed to remove oil by using alcohol-benzene mixture solution under temperature and pressure of 90 °C and 5 MPa, until fluorescent are qualified. The salt in samples was removed by using methanol extraction for 4 hr and soaked with distilled water. Finally, samples were dried at 105 °C until weight was unchanged. The porosity, vertical, and lateral permeability was measured with nitrogen under formation temperature and pressure, and porosity was calculated through gaseous state formula with error of 1%, and vertical and lateral permeability was measured using extrusion curves of Darcy's Law.

Another 36 representative core samples, including 18 fractured cores and 18 juxtaposed none-fracture cores, were prepared to perform pressure-controlled mercury injection (PMI) to study pore-throat geometry of dual media and matrix. These samples were cut into small cylinders 2.54 cm in diameter and 4 cm in length. AutoPoreIV9505 mercury porosimeter was used for this test following the standard SY/T 5346-2005 of China. The measurements were carried out at a temperature of 16 °C, a humidity of 50%. A mercury porosimeter is used to force mercury into all available space and measure entered mercury volume (Ziarani & Aguilera, 2012). Intrusion

and extrusion curves as well as various key parameters were obtained, such as average pore-throat radius, maximum pore-throat radius, and maximum mercury intrusion saturation. Notably, the PMI might have missed larger pores, although it can reasonably characterize pore-throats smaller than 63 μm , which shows the methods in ability to characterize the whole range of pore structures present in tight sandstone reservoirs (Zhao et al., 2015).

4 | RESULT

4.1 | Natural fracture occurrence in tight-sand reservoir

Generally, fractures in J_{1a} tight-sand reservoir are heterogeneous in size patterns (Figure 3). Fracture observation from core and FMI image suggests that natural fractures are primarily shear fractures. Fractures at a high angle to bedding (mostly subvertical) are present in core samples (Figure 3a,b), occurring that are inclined at ~ 70 to 80° to bedding. Of all core samples examined, subvertical fractures were observed in all 24 with small proportions of bedding-parallel fractures. Observation suggests that these macro-fractures from cores vary significantly in size. Specifically, their apertures vary from several hundreds to several thousands of microns; however, their lengths generally range from several centimetres to a few tens of centimetres

(Table 1). Also, typical opening-mode fracture configurations are dominated in most samples (Figure 3d and Table 1) with only several bitumen-sealed fractures (Figure 3c). Fractures may terminate abruptly at other fractures, or they may gradually taper (Figure 3b,c). Micro-fractures from thin sections are mostly parallel with each other, although vary significantly in length (Figure 3e,f). In terms of generation mechanisms, these multi-scale fractures can be explained with local and regional stress changes associated with tectonic activities, especially the Himalayan tectonic movement (Zeng et al., 2010; Zeng & Liu, 2006).

4.2 | Petrophysical properties

Generally, J_{1a} tight-sand reservoir is characterized by poor porosity, because measured helium porosity primarily ranges from 2% to 14%, with an average value of 7.7% (Figure 4a), whereas different from classic tight-sand reservoir around the world, J_{1a} tight-sand reservoir is not characterized by low-permeability, because measured permeability varies from 0.01–100 mD (Figure 4b), and over 37.9% permeability higher than 1 mD.

Thin-sections observation suggests three major types of pores in J_{1a} tight sandstone reservoirs, including interparticle dissolution pore, intragranular dissolution pore, and pore related to microfractures. The interparticle dissolution pores are commonly developed in J_{1a} tight-sand reservoir (Figure 5a–b), which were modified by mechanical compaction and cementation. The pore size varies between 20 and

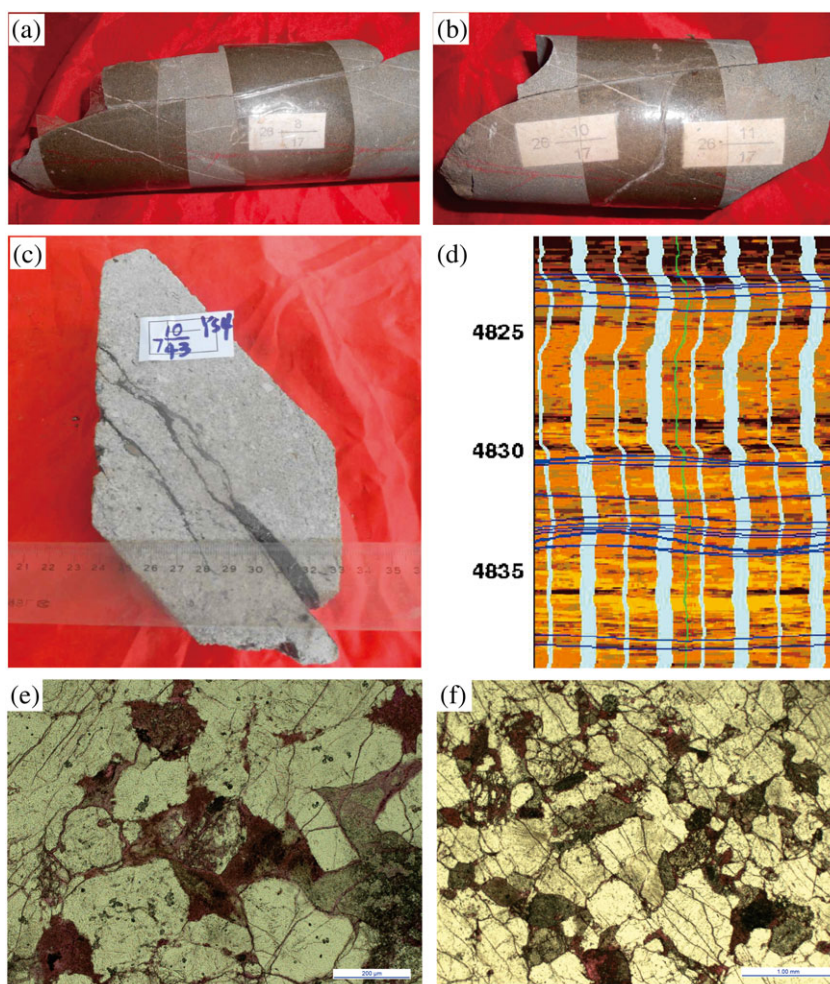
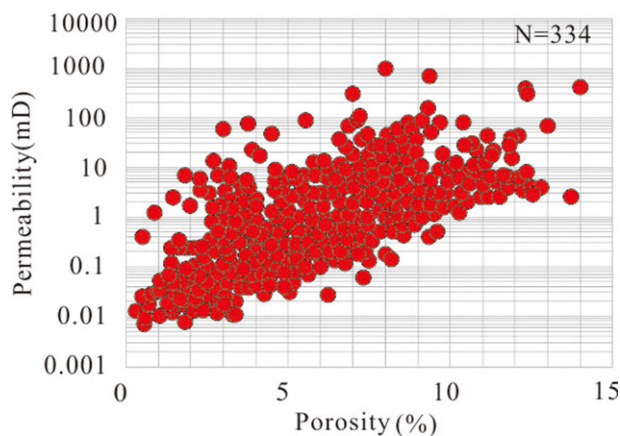


FIGURE 3 Photomicrograph, FMI image and thin-sections illustrating fractures at various scales in J_{1a} low-permeability reservoirs. (a) Inclined macro-fractures in J_{1a} tight-sand core from Yinan 2 well. (b) Termination of one fracture against another inclined one that dips steeply in similar direction from Yinan 2 well. (c) Steeply dipping, bitumen-sealed fractures in Yishen 4 well. (d) Fractures from Dixi 1 well are visible in an image log (marked by blue line), demonstrating they are open in reservoirs. (e) Well Yinan 4, 4379.25 m, coarse sandstone, large quartz crystal with breakage, and micro-fractures. (f) Well Yinan 5, 4844.06 m, coarse sandstone, having broken along micro-fractures, and numerous parallel fractures with large extension [Colour figure can be viewed at wileyonlinelibrary.com]

TABLE 1 Summary of fractures observed in cores from Yinan 2 tight-sand reservoir

Well	Formation	Depth(m)	Lithology	Aperture(mm)	Length(cm)	Filling characteristics
Yinan 2	J1a	4839.10–4843.30	Medium-coarse sandstone	0.1–0.5	9–41	Uncharged
Yinan 2	J1a	4896.87–4902.00	Fine-grained sandstone	0.4–0.9	8–27	Uncharged
Yinan 2	J1a	4964.04–4967.20	Fine-grained sandstone	0.3–0.5	12–30	Uncharged
Yinan 2	J1a	4412.21–4418.19	Fine-grained sandstone	0.1–1.5	11–29	Uncharged
Yinan 2	J1a	4559.00–4563.80	Coarse sandstone gravel	0.1–0.2	7–36	Uncharged
Yinan 2	J1a	4773.13–4779.00	Coarse sandstone	0–0.1	14–35	Uncharged
Yinan 2	J1a	4101.00–4105.20	Fine-grained sandstone	0.1–0.4	30–45	Uncharged

**FIGURE 4** The characteristics of reservoir property in J_{1a} sandstones. A. Porosity distribution. B. Permeability distribution [Colour figure can be viewed at wileyonlinelibrary.com]

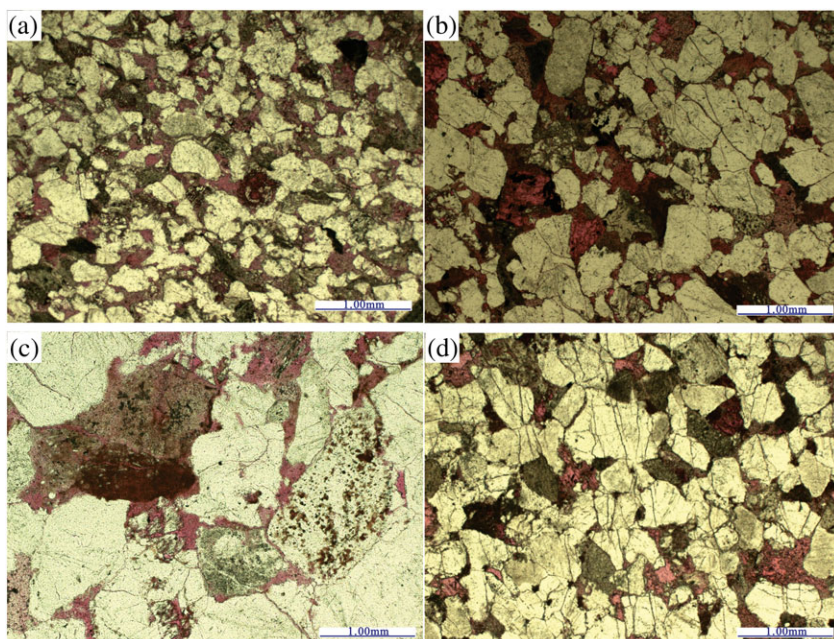
500 μm . Besides, intragranular dissolution pores occur mainly within clay minerals (Figure 5c) and partly dissolved feldspars (Figure 5d). The size of intragranular dissolution pores in clay minerals are typically about 50 to 1,000 μm , whereas feldspar intragranular dissolution pores are extremely small in size, ranging from 50 to 300 μm . Pores related to microfractures are mainly associated with brittle detrital grains (Figure 3e,f).

4.3 | Dual media in tight-sand reservoir

Based on fracture observation and petrophysical property analysis, full diameter core analysis, and conventional core analysis were conducted to systematically describe the characteristic of dual media in tight-sand reservoir.

The comparison between full diameter core analysis and conventional core analysis suggests that fractures in tight sandstones improve permeability significantly with only minor impact on storage space (Figure 6). Specifically, the ratio of permeability between dual media and tight sandstone is up to 1,000, whereas ratio of porosities only ranges from 1 to 1.5. In other words, fractures in dual media represent the high permeability system and make little contribution to pore volume, and the host rock constitutes primarily storage system and ultra-low permeability.

PMI results shows that the intrusion and extrusion curve patterns of typical samples vary with the increasing pressure (Figure 7). For none-fracture samples, displacement pressure, a threshold value forcing mercury to firstly inject into the rock, is commonly higher than 1 MPa, and the capillary pressures of mercury intrusion curves increase slowly at the first stage and are characterized by a horizontal trend (Figure 7a), indicating fine-sorted pore-throat and fine skewness rock samples. However, intrusion and curve pattern in Figure 7b differs markedly with that in Figure 7a and indicates poor-sorted and coarse

**FIGURE 5** Thin sections show typical pores in J_{1a} tight-sand reservoir. The red represents pores. (a) Yinan 5 well, 4770.78, fine sandstone, and interparticle dissolution pore. (b) Yishen 4 well, 3988.5, coarse sandstone, poor sorted, interparticle dissolution pore, tight grain arrangement, and lineal to concavo-convex grain contacts indicate strong compaction. (c) Yishen 4 well, 3997.62, dissolved clay minerals, and intragranular dissolution pore. (d) Yinan 2 well, 4545.10, coarse sandstone with strong compaction, and intra-granular dissolution pore [Colour figure can be viewed at wileyonlinelibrary.com]

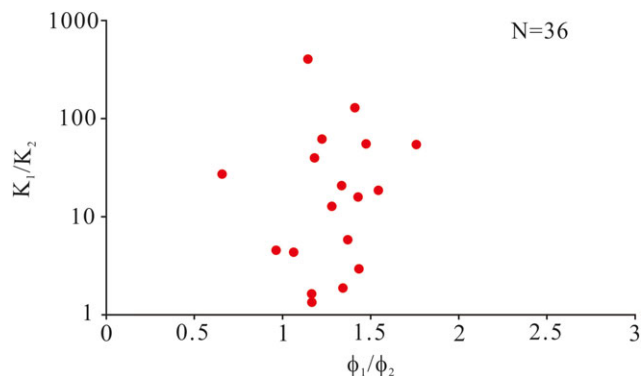


FIGURE 6 The comparison of porosity and permeability between dual media and tight-sand rocks, suggesting the improvement of porosity and permeability derived from dual media. Φ_1 and K_1 are result from dual media, and Φ_2 and K_2 are result from tight-sand rocks [Colour figure can be viewed at wileyonlinelibrary.com]

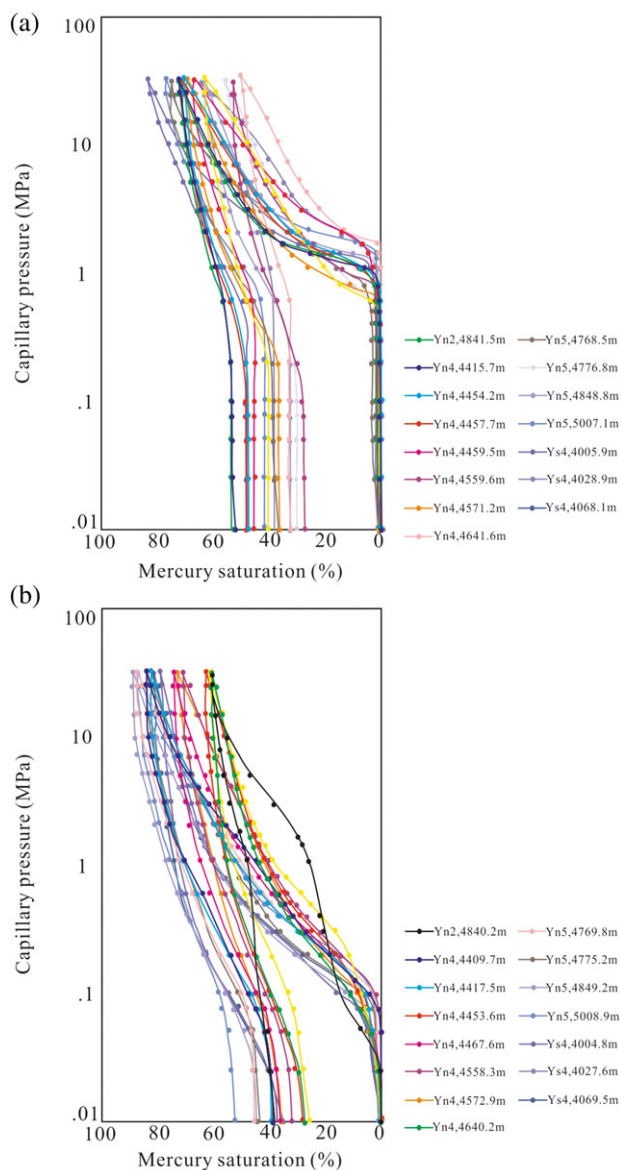


FIGURE 7 Intrusion and extrusion curves of pressure-controlled mercury injection. (a) None-fractured samples. (b) Fractured samples [Colour figure can be viewed at wileyonlinelibrary.com]

skewness samples, typical of dual media. Specifically, displacement pressure varies around 0.1 MPa, significantly lower than that of non-fracture samples. For example, the displacement pressure of dual media in Yinan 2 at 4840.2 m is only 0.031 MPa, which is remarkably lower than 1.446 MPa in juxtaposed tight-sand rocks in 4841.5 m. In addition, capillary pressure increases dramatically without readily noticeable horizontal trends (Figure 7b). Importantly, mercury intrusion curve from Yinan 2 at 4840.2 m (marked by black line in Figure 7b) indicates that the intrusion curve of dual media is characterized by “double peaks,” which can be divided into two sections by an obvious inflection point: The first section of the curve is marked by capillary pressure of 0.01–0.1 MPa, and the second section ranges from 0.1 to 32.1 MPa. Previous study (Yang, 2004) suggested that the first section of typical dual media is determined by fractures, and the second one is controlled by matrix pores.

The average pore-throat radius of tight-sand rocks ranges from 0.10 to 0.35 μm and the most frequent ones are populated mainly between 0.25 and 0.30 μm (Figure 8a), and the average pore-throat radius of dual media is over 0.40 μm with non-uniform frequency distribution (Figure 8b).

The maximum pore-throat radius (R_{m1}) of tight-sand rocks almost follows normal distribution, ranging from 0.40 to 1.20 μm with the most frequent value of 0.6 and 1.0 μm (Figure 8c), whereas the maximum pore-throat radius (R_{m2}) of dual media varies widely with non-uniform frequency distribution (Figure 8d). Moreover, the relative scattered distributions illustrate the complex and heterogeneous pore-throat size in dual media. The ratio between R_{m2} from dual media and R_{m1} from juxtaposed tight-sand rocks is 1.75–32.22, with an average value of 14.43. Thus, fractures can improve pore-throat radius of tight-sand rocks greatly, because R_{m2} can generally represent the fractures width in samples.

Furthermore, over 70% of the maximum mercury saturations (values corresponding to maximum injection capillary pressure) of tight-sand rocks is in a range of 60–85%, and 70% of the value of dual media ranges from 70 to 90% (Figure 8e,f). This comparison illustrates that fractures in dual media can make some contribution to pore volumes in tight-sand reservoir.

The medium saturation pressure, P50, the point on curve where the mercury intrusion saturation is 50%, is also different from tight-sand rocks and dual media. In general, the P50 of the tight-sand rocks are higher than 2 MPa (Figure 8g), whereas values of the dual media are one order lower than the former with a range of 0–0.8 MPa (Figure 8f).

Pore-throat size distribution and permeability contribution curves were calculated from pressure-controlled mercury injection results (Washburn, 1921). The results show that pore-throat radii of tight-sand rocks distribute in a narrow zone with two peaks. The pore-throat radii mainly centres on 0.01 to 1 μm , and radii of 0.1 to 1 μm contribute significantly to the permeability (Figure 9a). This might indicate that the pore throat size less than 0.1 μm may have limited influence on rock properties of tight sand rocks. However, different from tight-sand rocks, the pore-throat size distributed widely in dual media, with a range of 0.02–20 μm (Figure 9b). Also, pore-throat radii curve is characterized by three distinct peaks: one main peak accompanied by two minor peaks, indicating that the dual media is dominated by

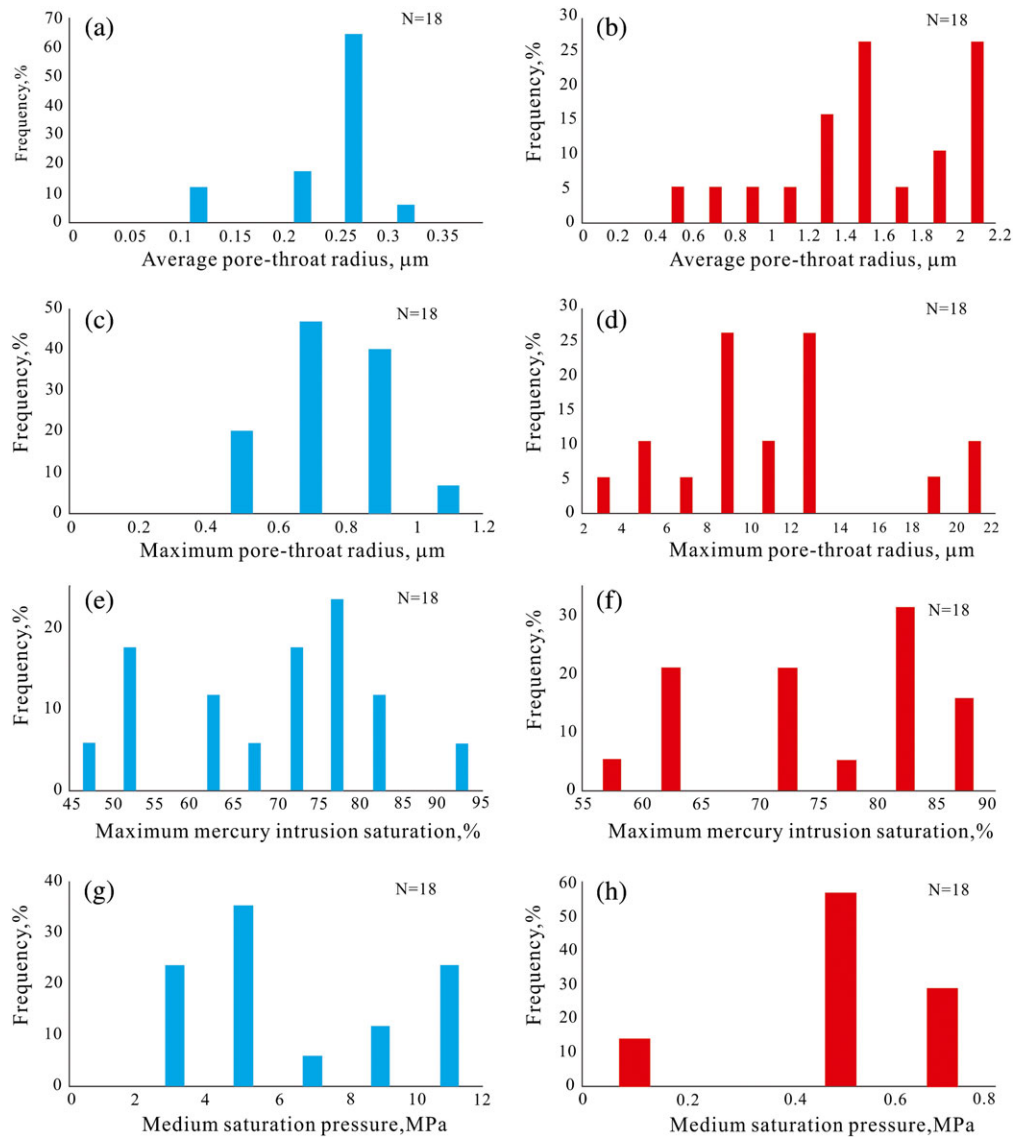


FIGURE 8 The parameters derived from pressure-controlled mercury injection experiments. (a,c,f,g) are parameters from tight-sand rocks, and (b,d,f,h) are from dual media. The “frequency” on the y-axis represents the sample ratio of each value intervals [Colour figure can be viewed at [wileyonlinelibrary.com](https://onlinelibrary.com)]

narrow pore throat (0.02–1 μm) with a small proportion of large pore throat (1–20 μm). Furthermore, although large pore throat is not the primarily throat in dual media, permeability varies significantly as a function of it, and is attributed negligibly to narrow pore throat. Thus, the comparison of pore-throat size distribution between tight-sand rock and dual media suggests that, once large pore throat occurs in rocks, it can determine permeability.

5 | DISCUSSION

Pressure-controlled mercury injection, full diameter core analysis, and conventional core analysis mentioned above suggest that the dual media associated with fractures and matrix pores can improve rock property significantly, which is favourable for hydrocarbon storage and migration. As shown in Figure 8a–f, pore-throat of fractured samples is much larger than those from non-fracture samples. And these large pore throats are responsible for the high permeability in

dual media (Figure 9), and make the dual media much more permeable than the matrix. This can explain the ratio of permeability between dual media and tight sandstone is up to 1,000. Furthermore, large pore throat in dual media can lower the resistance for gas migration, which makes natural fractures can be the main flow system in dual media and exert a positive effect on fluid flow in tight-sand rocks. On the other hand, compared with fractures, matrix pores contribute greatly to pore volume in dual media, which constitute the primary storage system in dual media. Therefore, the co-existence of fracture and matrix pores is favourable for gas migration and accumulation in dual media. This model is similar with previous studies that have emphasized the importance of fractures as fluid-flow pathways in conventional or unconventional reservoirs, such as carbonate reservoir and shale (Curtis, 2002; Gale, Laubach, Olson, Eichhubl, & Fall, 2014; Jarvie et al., 2003; Warren & Root, 1963; Guerriero et al., 2013).

Previous studies on gas migration dynamics held that almost no buoyancy exists in tight-sand gas reservoir (Berkenpas, 1991; Gies, 1981). Specifically, a theoretical model proposed by Berkenpas

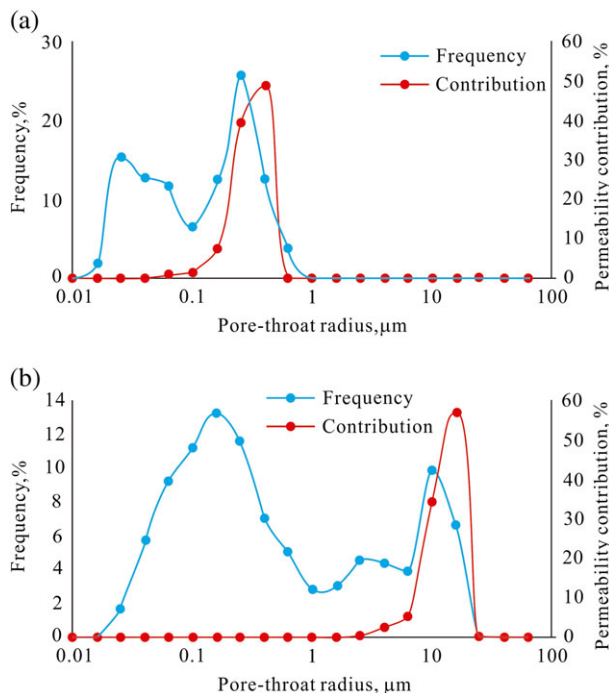


FIGURE 9 Pore-throat size distributions by pressure-controlled mercury injection of tight-sand rock from Yinan 2 well, 4841.5 m (a) and dual media from Yinan 2 well, 4840.2 m (b) [Colour figure can be viewed at wileyonlinelibrary.com]

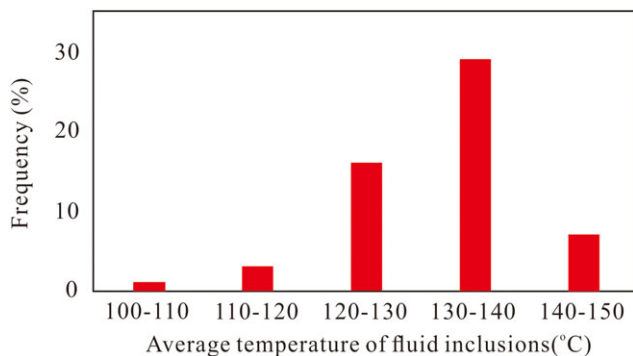


FIGURE 10 Modelled gas generation rate of T3t intervals and geotemperature history Yinan 2 well from Wang et al., (2016) [Colour figure can be viewed at wileyonlinelibrary.com]

(1991) suggested that force derived from pressure differential acts as a primary driving force for gas migration in tight-sand reservoir defined by critical throat threshold, whereas buoyancy was the main driving force in pores beyond the critical threshold. In terms of dual media in tight-sand reservoir, maximum pore-throat radius derived from fracture are much larger than that of matrix pores (ratio between R_{m2} and R_{m1} up to 32.22), which can result in multi migration force working together in dual media. Specifically, buoyancy can be the primary driving force when gas was charged from source rocks to reservoir through fractures, whereas pressure differential can motivate the migration after gas was charged into matrix pores.

As mentioned in the introduction section, many mechanisms have been put forwarded to explain the accumulation of tight-sand gas. However, formation mechanism of tight-sand gas in dual media may be totally different from typical tight sand reservoirs, which involves the position of dual media occurrence and the temporal coupling of dual media and gas charge in tight sand reservoirs (Wang et al., 2014). In the case of dual media occurrence prior to gas charge, fractures can be the dominant migration pathways, because the capillary pressure in fractures are smaller than that in matrix pores, and buoyancy is the primary driving force in fractures. And in this model, fractures may work as a flow system and matrix pores may work as storage system linked by fractures, which is favourable for gas accumulation in dual media. However, it may be difficult to form “inverted gas–water” in this model. In the case of gas charge prior to dual media occurrence, due to the lower pressure in fractures, gas may migrate from matrix pores to fractures. And fractures may destroy the “inverted gas–water” in the original tight-sand gas reservoir and result in shrinkage of tight-sand gas reservoir, because the increased pore throat cannot meet the requirement of critical throat threshold and destroy the dynamic balance (Berkenpas, 1991; Guo, Pang, Li, Guo, & Song, 2017). 1D hydrocarbon generation modelling from Wang et al. (2016) suggested that gas charging in J_{1a} tight-sand reservoir occurred from 90 °C, with an assumption that no obvious second migration occurred between J_{1a} tight-sand reservoir and adjacent T_{3t} source rocks (Figure 10). The homogenization temperature of fluid-inclusions in micro-fractures (Figure 11) indicates that fractures play a significant role in gas charging from 120 to 150°C. Thus, the gas charge in J_{1a} tight-sand reservoir was prior to the growth of fractures in Yinan 2

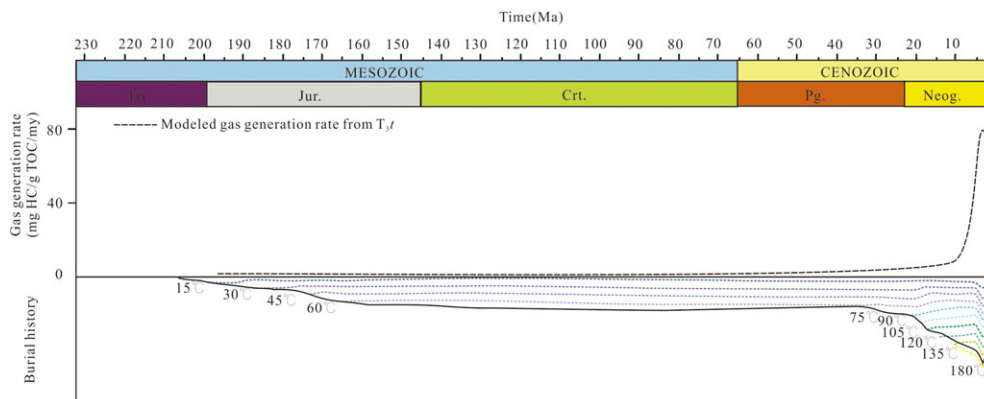


FIGURE 11 The homogenisation temperature of fluid-inclusions in micro-fractures in J_{1a} tight-sand reservoir from Wang (2016) [Colour figure can be viewed at wileyonlinelibrary.com]

well. In this case, the occurrence of dual media in J_1a tight-sand reservoir can exert a positive impact on gas charging in the inner part of the reservoir defined by the critical throat threshold. This can be evidenced by the high production from Yinan 2 well. However, dual media may have a negative effect on tight-sand gas reservoir when it occurs at the original critical throat threshold of Yinan 2 tight-sand reservoir (Wang et al., 2014). However, to clarify the impact of deal media on tight-sand gas accumulation, more evidence will be expected in the future.

6 | CONCLUSION

1. Subvertical fractures are widely distributed in Ahe Formation (J_1a) tight sandstones, with dip angle of 70° to 80° . These fractures are strongly scale-dependent, with a length of several centimetres to a few tens of centimetres and apertures of several hundreds to several thousands of microns. J_1a tight-sand reservoir is characterized by poor porosity, with an average value of 7.7%, whereas measured permeability varies from 0.01–100 mD.
2. Intrusion and extrusion curves of dual media and tight-sand rocks are significantly different between each other, although displacement pressures and medium saturation pressure of dual media are lower than these of tight-sand rocks. Importantly, maximum pore throats of dual media are 1.75–32.22 times larger than that of juxtaposed tight-sand rocks. The ratio of permeability between dual media and tight sandstone is up to 1,000, whereas the ratio of porosities only ranges from 1 to 1.5. Thus, fractures in dual media represent the high permeability system and the matrix pores are primarily storage system.
3. Gas charging and accumulating in dual media remarkably differ from typical tight-sand reservoir, because dual media has high permeability system, which can lower resistance for gas migration. Also, the impact of dual media on tight-sand gas reservoir involves its position and temporal coupling of gas charging and dual media growth. In terms of fracture growth prior to gas charge, multi-force can work together as the driving force, and fractures as a flow system and matrix pores as a storage system linked by fractures; buoyancy is the primary driving force in fractures. In terms of gas charge prior to fracture growth, dual media can also exert a positive impact on gas charging when dual media occurs in the inner part of tight-sand reservoir defined by the critical throat threshold. However, dual media may destroy the “inverted gas–water” and shrink tight-sand gas reservoir when it occurs at the original critical throat threshold.

ACKNOWLEDGEMENTS

We like to thank the Tarim Oilfield Exploration and Development Research Institute for providing geologic data. This study is financially supported by the China Postdoctoral fund (2017M610150) and China National Science and Technology Major Project (2016ZX05047-006). Executive Editor Zhong-Qiang Chen and two anonymous journal reviewers are also thanked for their constructive comments and suggestions, which have improved greatly the quality of the paper.

ORCID

Pengwei Wang  <http://orcid.org/0000-0001-9057-3723>

REFERENCES

- Aguilera, R. (1995). *Naturally fractured reservoirs* (2nd ed.). (pp. 505). Tulsa, Oklahoma: PennWell Books.
- Anovitz, L. M., Cole, D. R., Rother, G., Allard, L. F., Jackson, A. J., & Littrell, K. C. (2013). Diagenetic changes in macro-to nano-scale porosity in the St. Peter Sandstone: An (ultra) small angle neutron scattering and backscattered electron imaging analysis. *Geochimica et Cosmochimica Acta*, 102, 280–305.
- Bai, B., Zhu, R., Wu, S., Yang, W., Jeff, G., Allen, G., ... Su, L. (2013). Multi-scale method of Nano(Micro)-CT study on microscopic pore structure of tight sandstone of Yanchang Formation, Ordos Basin. *Petroleum Exploration and Development*, 40, 354–358 (in Chinese, English abstract).
- Berkenpas, P. G. (1991). The Milk River shallow gas pool: Role of the updip water trap and connate water in gas production from the pool. *SPE*, 22922, 371–380.
- Cant, D. (1983). Spirit River Formation: A stratigraphic-diagenetic gas trap in the deep basin of Alberta. *AAPG Bulletin*, 67, 577–587.
- Chen, Z., Lavoie, D., Malo, M., Jiang, C., Sanei, H., & Ardakani, O. H. (2017). A dual-porosity model for evaluating petroleum resource potential in unconventional tight-shale plays with application to Utica Shale, Quebec (Canada). *Marine and Petroleum Geology*, 80, 333–348.
- Chen, Z. Q., & Shi, G. R. (2003). Late Paleozoic depositional history of the tarim basin, Northwest China: An integration of biostratigraphic and lithostratigraphic constraints. *AAPG Bulletin*, 87, 1323–1354.
- Chen, S. P., Tang, L. J., Jin, Z. J., Jia, C. Z., & Pi, X. J. (2004). Thrust and fold tectonics and the role of evaporites in deformation in the Western Kuqa Foreland of Tarim Basin Northwest China. *Marine and Petroleum Geology*, 21, 1027–1042.
- Chilingar, G. V., Mannon, R. W., & Rieke, H. H. I. (1972). Oil and gas production from carbonate rocks. *American Elsevier Publishing Company Inc New York*, 96, 86–91.
- Cluff, R. M., Shanley, K. W., & Byrnes, A. P. (2005). Permeability jail and implications for “basin centered gas” production and resource assessment. *AAPG Search and Discovery*.
- Coskun, S. B., & Wardlaw, N. C. (1996). Image analysis for estimating ultimate oil recovery efficiency by waterflooding for two sandstone reservoirs. *Journal of Petroleum Science and Engineering*, 15, 237–250.
- Curtis, J. B. (2002). Fractured shale-gas systems. *AAPG Bulletin*, 86, 1921–1938.
- Dai, J. X., Ni, Y. Y., & Wu, X. Q. (2012). Tight gas in China and its significance in exploration and exploitation. *Petroleum Exploration and Development*, 39, 257–264 (in Chinese, English abstract).
- Desbois, G., Urai, J. L., Kukla, P. A., Konstanty, J., & Baerle, C. (2011). High-resolution 3D fabric and porosity model in a tight gas sandstone reservoir: A new approach to investigate microstructures from mm-to nm-scale combining argon beam cross-sectioning and SEM imaging. *Journal of Petroleum Science and Engineering*, 78, 243–257.
- Ding, D. G., & Luo, Y. M. (2005). Collision structures in Pamir region and reformation of Tarim Basin. *Oil and Gas Generation*, 26, 57–63 (in Chinese, English abstract).
- Fan, Q. H., Lu, X. X., Yang, M. H., & Xie, H. W. (2008). Influence of salt beds on the segmentation of structure and hydrocarbon accumulation in Qulitag Structural Belt, Tarim Basin, China. *Journal of China University of Geosciences*, 19, 162–173 (in Chinese, English abstract).
- Fu, X. F., Song, Y., Lü, Y. F., & Sun, Y. H. (2006). Rock mechanic characteristic of gypsum cover and conservation function to gas in the Kuche Depression, the Tarim Basin. *Petroleum Geology & Experiment*, 28, 25–29.
- Gale, J. F., Laubach, S. E., Olson, J. E., Eichhubl, P., & Fall, A. (2014). Natural fractures in shale: A review and new observations. *AAPG Bulletin*, 98, 2165–2216.

- Gao, R. Q., & Zhao, Z. Z. (2001). *The frontier petroleum exploration in China-Exploration of the large gas field in Kuqa Depression of Tarim Basin* (pp. 112–114). Beijing: Petroleum industry press (in Chinese).
- Gies, R. M. (1981). Lateral trapping mechanisms in “Deep Basin” gas trap, western Canada (abs.). *AAPG Bulletin*, 65, 930.
- Gies, R. M. (1984). Case history for a major Alberta deep basin gas trap: The Cadomin formation. *AAPG Memoir*, 38, 115–140.
- Gu, J. Y., Zhu, X. M., & Jia, J. H. (2003). *Depositions and reservoirs in Tarim Basin* (pp. 400). Beijing: Petroleum Industry Press (in Chinese).
- Guerriero, V., Mazzoli, S., Iannace, A., Vitale, S., Carravetta, A., & Strauss, C. (2013). A permeability model for naturally fractured carbonate reservoirs. *Marine and Petroleum Geology*, 40, 115–134.
- Guo, Y., Pang, X., Li, Z., Guo, F., & Song, L. (2017). The critical buoyancy threshold for tight sandstone gas entrapment: Physical simulation, interpretation, and implications to the Upper Paleozoic Ordos Basin. *Journal of Petroleum Science and Engineering*, 149, 88–97.
- Hinai, A., Rezaee, R., Esteban, L., & Labani, M. (2014). Comparisons of pore size distribution: A case from the Western Australian gas shale formations. *Journal of Unconventional Oil and Gas Resources*, 8, 1–13.
- Jarvie, D. M., Hill, R. J., Pollastro, R. M., Wavrek, D. A., Bowker, K. A., Claxton, B. L., & Tobey, M. H. (2003). Evaluation of unconventional natural gas prospects: The Barnett Shale fractured shale gas model. In 21st International Meeting on Organic Geochemistry.
- Jia, C. (1997). *Tectonic characteristics and petroleum Tarim Basin China*. (pp. 56–58). Beijing: Petroleum industry press.
- Jia, D., Lu, J., & Cai, D. (1998). Structural features of northern Tarim Basin: Implications for regional tectonics and petroleum traps. *AAPG Bulletin*, 82, 147–159.
- Jia, C., Zheng, M., & Zhang, Y. (2012). Unconventional hydrocarbon resources in China and the prospect of exploration and development. *Petroleum Exploration and Development*, 39, 139–146.
- Landes, K. K. (1959). *Petroleum geology* (2nd ed.). (pp. 169). John Wiley and Sons Inc.
- Liu, Z., Lu, H., Li, X., Jia, C., Lei, G., Chen, C., ... Fan, X. (2000). Structural evolution of Kuqa re-generated Foreland Basin. *Geological Science*, 35, 482–492 (in Chinese, English abstract).
- Lyu, W., Zeng, L., Zhang, B., Miao, F., Lyu, P., & Dong, S. (2017). Influence of natural fractures on gas accumulation in the Upper Triassic tight gas sandstones in the northwestern Sichuan Basin, China. *Marine and Petroleum Geology*, 83, 60–72.
- Masters, J. A. (1979). Deep basin gas trap, Western Canada. *AAPG Bulletin*, 63, 152–181.
- Pang, X. Q., Jin, Z. J., & Jiang, Z. X. (2003). Critical condition for gas accumulation in the deep basin trap and physical modeling. *Natural Gas Geoscience*, 14, 207–214 (in Chinese, English abstract).
- Rezaee, R., Saeedi, A., & Clennell, B. (2012). Tight gas sands permeability estimation from mercury injection capillary pressure and nuclear magnetic resonance data. *Journal of Petroleum Science and Engineering*, 88, 92–99.
- Shanley, K. W., & Cluff, R. M. (2015). The evolution of pore-scale fluid-saturation in low permeability sandstone reservoirs. *AAPG Bulletin*, 99, 1957–1990.
- Tang, L. J., Jia, C. Z., Jin, Z. J., Chen, S. P., Pi, X. J., & Xie, H. W. (2004). Salt tectonic evolution and hydrocarbon accumulation of Kuqa foreland fold belt, Tarim Basin, NW China. *Journal of Petroleum Science and Engineering*, 41, 97–108 (in Chinese, English abstract).
- Wang, P. W. (2016). *The controlling of faults on hydrocarbon accumulations in deep basin and its mechanism in Kuqa Depression*. (pp. 78). China university of Petroleum (Beijing).
- Wang, P. W., Chen, X., Pang, X., Jiang, Z., Jiang, F., Guo, Y., ... Wen, J. (2014). The controlling of structure fractures on the accumulation of tight sand gas reservoirs. *Natural Gas Geoscience*, 25, 185–191.
- Wang, P. W., Pang, X. Q., Jiang, Z. X., Guo, Y. C., Chen, X., Wang, Y. W., & Jiao, J. (2016). Origin and evolution of overpressure in the Lower Jurassic succession in the Kuqa Depression, Western China. *Journal of Natural Gas Science and Engineering*, 28, 700–710.
- Wang, Z. Y. (2002). Physical and mechanical properties of mesozoic and cenozoic rocks in the west of Kuche depression in Tarim Basin. *Progress in geophysics*, 17, 399–405.
- Warren, J. E., & Root, P. J. (1963). The behavior of naturally fractured reservoirs. *Society of Petroleum Engineers Journal*, 3, 245–255.
- Washburn, E. W. (1921). The dynamics of capillary flow. *Physical Review*, 17, 273–283.
- Wei, G. Q., Zhang, F. D., Li, J., Yang, S., Huang, C. Y., She, Y. Q., ... Zhao, L. H. (2016). New progress of tight sand gas accumulation theory and favorable exploration zones in China. *Natural Gas Geoscience*, 27, 199–210 (in Chinese, English abstract).
- Xiao, Z. H., Zhong, N. N., Huang, Z. L., Jiang, Z. X., & Liu, Y. (2008). A study on hydrocarbon pooling conditions in tight sandstones through simulated experiments. *Oil & Gas Geology*, 29, 721–725 (in Chinese, English abstract).
- Yang, S. (2004). *Reservoir physics*. (pp. 76–80). Beijing: Petroleum industry press.
- Yin, A., & Harrison, T. M. (2003). Geologic evolution of the himalayan-tibetan orogen. *Annual Review of Earth & Planetary Sciences*, 28, 211–280.
- Yin, A., Rumelhart, P. E., Butler, R., Cowgill, E., Harrison, T. M., & Foster, D. A. (2002). Tectonic history of the altyn tagh fault system in northern tibet inferred from cenozoic sedimentation. *Geological Society of America Bulletin*, 114, 1257–1295.
- Zeng, L. B. (2004). Characteristics and petroleum geological significance of Himalayan orogeny in Kuqa foreland basin. *Oil & Gas Geology*, 25, 175–179 (in Chinese, English abstract).
- Zeng, L. B., & Liu, B. M. (2006). Abnormal high pressure in Kuqa foreland thrust belt of Tarim Basin: Origin and impacts on hydrocarbon accumulation. *Progress in Natural Science*, 16, 1307–1314.
- Zeng, L. B., Wang, H. J., Gong, L., & Liu, B. M. (2010). Impacts of the tectonic stress field on natural gas migration and accumulation: A case study of the Kuqa Depression in the Tarim Basin, China. *Marine and Petroleum Geology*, 27, 1616–1627.
- Zhang, L. P., Bai, G. P., Luo, X. R., Ma, X. H., Chen, M. J., Wu, M. H., & Yang, W. X. (2009). Diagenetic history of tight sandstones and gas entrapment in the Yulin Gas Field in the central area of the Ordos Basin, China. *Marine and Petroleum Geology*, 26, 974–989.
- Zhao, H., Ning, Z., Wang, Q., Zhang, R., Zhao, T., Niu, T., & Zeng, Y. (2015). Petrophysical characterization of tight oil reservoirs using pressure-controlled porosimetry combined with rate-controlled porosimetry. *Fuel*, 154, 233–242.
- Ziarani, A. S., & Aguilera, R. (2012). Pore-throat radius and tortuosity estimation from formation resistivity data for tight-gas sandstone reservoirs. *Journal of Applied Geophysics*, 83, 65–73.
- Zou, C., Jia, J., Tao, S., & Tao, X. (2011). Analysis of reservoir forming conditions and prediction of continuous tight gas reservoirs for the deep Jurassic in the eastern Kuqa Depression, Tarim basin. *Acta Geologica Sinica (English Edition)*, 85, 1173–1186.
- Zou, C. N., Yang, Z., Tao, S. Z., Yuan, X. J., Zhu, R. K., Hou, L. H., ... Pang, Z. L. (2013). Continuous hydrocarbon accumulation over a large area as a distinguishing characteristic of unconventional petroleum, The Ordos Basin, North-Central China. *Earth-Science Reviews*, 126, 358–369.
- Zou, C. N., Zhu, R. K., Liu, K. Y., Su, L., Bai, B., Zhang, X. X., ... Wang, J. H. (2012). Tight gas sandstone reservoirs in China: Characteristics and recognition criteria. *Journal of Petroleum Science and Engineering*, 88–89, 82–91.

How to cite this article: Wang P, Jin Z, Pang X, Guo Y, Chen X, Guan H. Characteristics of dual media in tight-sand gas reservoirs and its impact on reservoir quality: A case study of the Jurassic reservoir from the Kuqa Depression, Tarim Basin, Northwest China. *Geological Journal*. 2017;1–11. <https://doi.org/10.1002/gj.3091>